Acta Crystallographica Section F
Structural Biology and Crystallization Communications
ISSN 1744-3091

Structure of the P_{II} signal transduction protein of *Neisseria meningitidis* at 1.85 Å resolution

Charles E. Nichols,[a] Sarah Sainsbury,[b] Nick S. Berrow,[b] David Alderton,[b] Nigel J. Saunders,[c] David K. Stammers[a,b] and Raymond J. Owens[b]*

[a]Division of Structural Biology, Henry Wellcome Building for Genomic Medicine, University of Oxford, Roosevelt Drive, Oxford OX3 7BN, England, [b]The Oxford Protein Production Facility, Henry Wellcome Building for Genomic Medicine, University of Oxford, Roosevelt Drive, Oxford OX3 7BN, England, and [c]The Bacterial Pathogenesis and Functional Genomics Group, The Sir William Dunn School of Pathology, University of Oxford, South Parks Road, Oxford OX1 3RE, England

Correspondence e-mail: ray@strubi.ox.ac.uk

Received 24 January 2006
Accepted 27 April 2006

PDB Reference: P_{II} signal transduction protein, 2gw8, r2gw8sf.

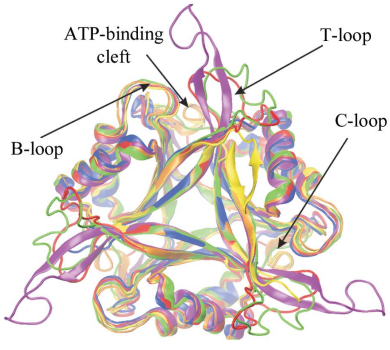

The P_{II} signal transduction proteins GlnB and GlnK are implicated in the regulation of nitrogen assimilation in *Escherichia coli* and other enteric bacteria. P_{II}-like proteins are widely distributed in bacteria, archaea and plants. In contrast to other bacteria, *Neisseria* are limited to a single P_{II} protein (NMB 1995), which shows a high level of sequence identity to GlnB and GlnK from *Escherichia coli* (73 and 62%, respectively). The structure of the P_{II} protein from *N. meningitidis* (serotype B) has been solved by molecular replacement to a resolution of 1.85 Å. Comparison of the structure with those of other P_{II} proteins shows that the overall fold is tightly conserved across the whole population of related proteins, in particular the positions of the residues implicated in ATP binding. It is proposed that the *Neisseria* P_{II} protein shares functions with GlnB/GlnK of enteric bacteria.

1. Introduction

The signal transduction protein P_{II} (GlnB) is best known for its role in the regulation of nitrogen assimilation in enteric bacteria. However, closely related proteins are found in a wide variety of organisms including bacteria, archaea and plants (Arcondeguy *et al.*, 2001; Ninfa & Jiang, 2005; Ninfa & Atkinson, 2000). In *Escherichia coli*, P_{II} and its paralogue GlnK, which is only induced under nitrogen limitation, are involved in two signalling pathways that regulate the activity of glutamine synthetase. Firstly, the bifunctional uridylyl-transferase/uridylyl-removing enzyme (UTase/UR, the product of *glnD*) uridylates a conserved tyrosine (Tyr51) of P_{II} under nitrogen-starvation conditions, whereas under circumstances of nitrogen excess the enzyme removes UMP from P_{II} (Jaggi *et al.*, 1996; Jiang *et al.*, 1998*a*). Native P_{II} activates the adenylation activity of ATase, which in turn inhibits glutamine synthetase, whilst UMP-P_{II} reverses this effect (Jaggi *et al.*, 1997; Mangum *et al.*, 1973). Secondly, P_{II} affects glutamine synthetase transcription by modulating the activity of the kinase/phosphatase NRII (the *ntrB* gene product), which controls the phosphorylation status of the transcription factor NRI (the *ntrC* gene product). In its phosphorylated form, NRI stimulates transcription of the glutamine synthetase gene, whilst the unphosphorylated NRI acts as a repressor. Native P_{II} binds to NRII, preventing phosphorylation of NRI and hence the activation of GS transcription (Liu & Magasanik, 1995). UMP-P_{II}, which is generated under nitrogen-limiting conditions through uridylation of the T-loop, which extends beyond an otherwise compact trimeric structure, does not bind NRII and hence activation of GS *via* phosphorylated NRI can proceed (Jiang *et al.*, 1998*b*). In addition, *E. coli* P_{II} binds cooperatively to two effectors, ATP and α-ketogluturate (Jiang *et al.*, 1998*a*). The binding of α-ketogluturate regulates the interaction between P_{II} and ATase, thus integrating signals from carbon and nitrogen metabolism.

Although in *E. coli* the P_{II} paralogue GlnK (van Heeswijk *et al.*, 1995, 1996) appears to have similar properties to P_{II} and can form heterotrimers with P_{II} (van Heeswijk *et al.*, 2000), GlnK also has distinct roles. In many bacteria, including *E. coli*, GlnK is associated with regulation of the *amtB* gene, which encodes the ammonium transporter (Coutts *et al.*, 2002). GlnK is also involved in the NifL–NifA regulatory system of nitrogen-fixing bacteria (Little *et al.*, 2000).

The X-ray crystal structures of both P_{II} (Cheah *et al.*, 1994; Xu *et al.*, 2001) and GlnK (Xu *et al.*, 1998) from *E. coli*, as well as a number of other P_{II} proteins [those from *Herbaspirillum seropedicae* (Machado Benelli *et al.*, 2002), *Synechoccus* sp. PCC7942 and *Synchocystis* sp. PCC6803 (Xu *et al.*, 2003), *Thermus thermophilus* (Sakai *et al.*, 2005) and *Thermotoga maritima* (Schwarzenbacher *et al.*, 2004)], have been solved. All share a highly conserved monomer structure arranged into a tightly associated trimer. A key feature of the structures is the so-called T-loop which contains the regulatory uridylylation site (Tyr51) or, in the case of cyanobacteria, a phosphorylation site (Ser49; Forchhammer & Tandeau de Marsac, 1995). The T-loop has been implicated in the protein–protein interactions of P_{II} in *E. coli* (Jiang, Zucker & Ninfa, 1997; van Heeswijk *et al.*, 2000; Martinez-Argudo & Contreras, 2002) and shows differences in conformation in the crystal structures.

Neisseria spp. are Gram-negative β-protobacteria which include many species found only in humans, including successful pathogens. In recent years, the genomes of *N. meningitidis* serotypes A (strain Z2491; Parkhill *et al.*, 2000) and B (strain MC58; Tettelin *et al.*, 2000) and *N. gonorrhoeae* (strain FA1090; currently unpublished work) have been sequenced and annotated. Each contain a single P_{II} protein encoded by a monocistronic operon (NMB1955 in *N. meningitidis* strain MC58). The three neisserial P_{II} proteins have 98% identical sequences and share 73% identity to the P_{II} from *E. coli*. As part of a structural proteomics approach to the study of *Neisseria*, we have solved the structure of P_{II} from *N. meningitidis* (gene locus NMB1995) to 1.85 Å resolution using the semi-automated pipeline of the Oxford Protein Production Facility (OPPF).

2. Materials and methods

Cloning, expression and protein purification followed standard OPPF pipeline protocols, as described previously (Ren *et al.*, 2005). Briefly, the P_{II} gene (NMB 1955) was amplified from genomic DNA by PCR with the forward primer ggggacaagtttgtacaaaaaagcaggcttcctggaagttctgttccagggcccgATGAAAAAAATCGAGGCGATTGTC and the reverse primer ggggaccactttgtacaagaaagctgggtctcaTCAGACTGCCGCGTCCGAAC incorporating an N-terminal His tag followed by a 3C protease-cleavage site and inserted into the expression vector pDEST17 using Gateway recombinatorial cloning (Invitrogen). Expression was induced by the addition of 0.5 m*M* IPTG and the protein was purified by a combination of Ni–NTA affinity chromatography and gel filtration. The N-terminal His tag was removed by cleavage with 3C protease prior to gel filtration. The protein was crystallized using the nanodrop crystallization procedure with standard OPPF protocols (Walter *et al.*, 2003). Hits from this initial screening exercise were then tested in-house using a MAR 345

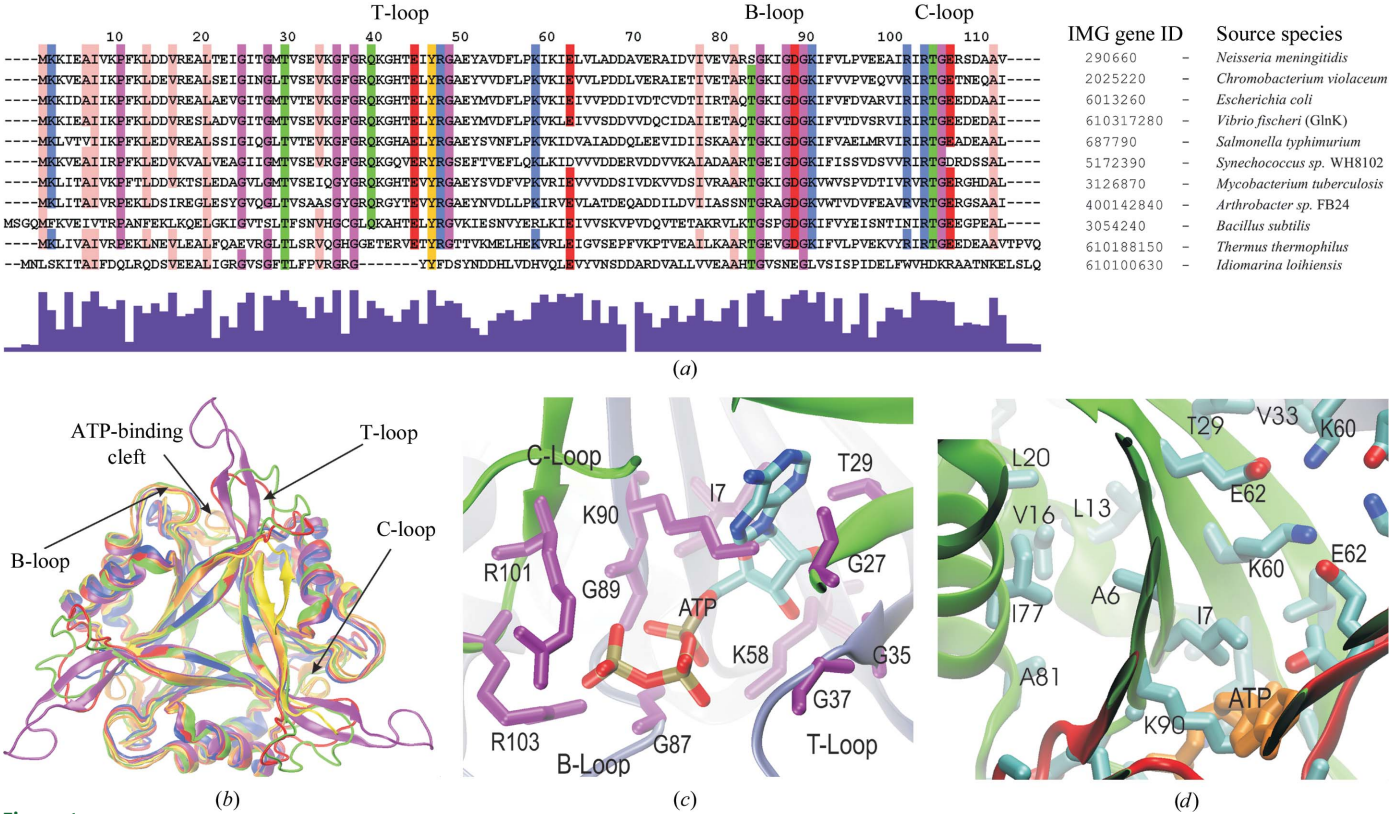

Figure 1

(*a*) *ClustalW* alignment of P_{II} paralogue protein sequences, numbered relative to the *N. meningitidis* P_{II} sequence, with the T-loop (amino acids 37–55), B-loop (amino acids 81–90) and C-loop (amino acids 96–112) marked. The alignment view was generated with *JALVIEW*, with colouring according to the Zappo colour scheme, but applied only to residues showing a population identity of ≥80%. (*b*) 'New-cartoon' format C^{α}-trace overlay of *N. meningitidis* P_{II} and five other selected P_{II} paralogue structures, illustrating tight conservation of the core region and the location of the B-, C- and T-loops relative to the ATP-binding cleft. *N. meningitidis* P_{II}, PDB code 2gw8, green; *E. coli* P_{II}/GlnB, PDB code 2pii, red; *E. coli* GlnK, PDB code 2gnk, orange; *H. seropedicae* GlnK, PDB 1hwu, yellow; *Synechococcus* sp. GlnB, PDB code 1qy7, purple; *T. thermophilus* TT021, PDB code 1v9o, dark blue. (*c*) 'New-cartoon' format C^{α} trace of *N. meningitidis* P_{II} coloured by chain showing a close-up view of the ATP-binding site, with conserved residues labelled according to the standard single-letter sequence code and displayed in 'liquorice' format coloured purple. ATP is also shown in 'liquorice' format coloured by name; the coordinates were derived from a C^{α}-trace overlay of *E. coli* ATP-bound structure PDB code 2gnk and *N. meningitidis* P_{II}. (*d*) Cutaway view 'new-cartoon' format C^{α}-trace of *N. meningitidis* P_{II} coloured by chain, with selected residues labelled according to the standard single-letter sequence code and displayed in 'liquorice' format and coloured by name, illustrating the central Lys60/Glu62 oligomerization contact and the conserved hydrophobic pocket. ATP is also shown in 'liquorice' format coloured orange, with coordinates derived from a C^{α}-trace overlay of *E. coli* ATP-bound structure PDB code 2gnk and *N. meningitidis* P_{II}.

Table 1
Data-collection and processing statistics.

Values in parentheses are for outer shell data.

Space group	$P6_3$
Unit-cell parameters (Å, °)	$a = b = 61.14$, $c = 48.07$, $\alpha = \beta = 90$, $\gamma = 120$
Resolution range	30.00–1.85 (1.92–1.85)
Redundancy	5.5 (5.4)
Completeness (%)	99.8 (100.0)
$R_{\rm merge}$†	0.065 (0.418)
$I/\sigma(I)$	28.1 (4.7)
No. of subunits in ASU	1
$R_{\rm work}$‡ (%)	17.7
$R_{\rm free}$‡ (%)	21.9
Residues in most favoured regions§ (%)	95.2
Residues in additionally allowed regions§ (%)	4.8
Mean *B* factors	
All atoms	34.0
Protein	
Main chain	22.7
Side chain	30.5
Water	55.6
R.m.s.d bond lengths (Å)	0.005
R.m.s.d. bond angles (°)	1.24

† $R_{\rm merge} = \sum|I_{\rm obs} - \langle I\rangle|/\sum\langle I\rangle$. ‡ $R = \sum_{hkl}|F_{\rm o}(hkl) - F_{\rm c}(hkl)|/\sum_{hkl}|F_{\rm o}(hkl)|$.
§ Ramachandran plot results from *PROCHECK*.

image-plate system on a Rigaku generator equipped with a Cu anode and Osmic multilayer optics, giving Cu $K\alpha$ radiation with $\lambda = 1.5418$ Å. The best diffraction observed ($d_{\rm min} < 2.0$ Å) was from a $75 \times 25 \times 25$ µm rod-shaped crystal grown in Hampton Cryo Screen I condition No. 31 [0.17 *M* ammonium sulfate, 25.5% PEG 4000, 15%(*v*/*v*) glycerol]. This crystal was therefore frozen and dry-shipped to Daresbury for data collection. Indexing, integration and merging of data images were carried out with *DENZO* and *SCALEPACK* (Otwinowski & Minor, 1997). Rotation-function searches, translation searches and initial rigid-body Patterson correlation refinement were carried out using *CNS* (Brünger *et al.*, 1998) and molecular-replacement solutions were checked by displaying the transformed coordinates in *O*, as described in Jones *et al.* (1991). Rigid-body, positional and *B*-factor refinement, simulated annealing and initial water picking were carried out in *CNS*. Manual rebuilding, including insertion of ions, ligands and extra water molecules, was carried out using the program *O*. Homologous sequences to *N. meningitidis* P_{II} were selected from the Integrated Microbial Genomes (IMG) database (http://img.jgi.doe.gov/cgi-bin/pub/main.cgi), aligned with *ClustalW* (Thompson *et al.*, 1994; Chenna *et al.*, 2003) and visualized using *JALVIEW* (Clamp *et al.*, 2004). Model quality was assessed using *PROCHECK* (Laskowski *et al.*, 1993). The final *N. meningitidis* P_{II} model was overlaid with the previously released GlnB and GlnK structures using *TOPP* (Collaborative Computational Project, Number 4, 1994) and the results were compared visually in *O* and *VMD* (Humphrey *et al.*, 1996). Final figures were prepared from *VMD* screenshots using *Corel*11.

3. Results and discussion

The structure of P_{II} from *N. meningitidis* was determined by molecular replacement using the PDB model 1pil (*E. coli* P_{II}) to a resolution of 1.85 Å (Table 1). As with the *E. coli* crystal structure, P_{II} from *N. meningitidis* has a single molecule in the asymmetric unit. Each molecule of the trimer (the normal biological oligomeric state) is therefore in a crystallographically equivalent environment, indicating that all three chains have the same conformational state. The flexible T-loop (residues 37–55) is semi-disordered from residues 38 to 52 in the *N. meningitidis* P_{II} crystal structure, although sufficient residual density was still visible in low-contoured difference maps (2.2σ $F_{\rm o} - F_{\rm c}$ density) to allow an approximate fit based on a rigid-body overlay of the T-loop from *E. coli* P_{II}. This section is thus included in Figs. 1(*b*), 1(*c*) and 1(*d*) for comparative purposes, but is omitted from the final deposited coordinates (PDB code 2gw8).

Comparing C^{α}-trace overlays of *N. meningitidis* P_{II} with five additional P_{II} structures obtained from the PDB, the mean C^{α} r.m.s.d. for the core section, excluding the flexible T-loop, is just 0.9 Å, with a range of 0.7–1.0 Å (Fig. 1*b*; *N. meningitidis* P_{II} is in green, *E. coli* P_{II}/GlnB is in red, *E. coli* GlnK is in orange, *H. seropedicae* GlnK is in yellow, *Synechococcus* sp. GlnB is in purple and *T. thermophilus* TT021 is in dark blue). The overall fold is thus very tightly conserved across the whole population of P_{II} proteins. The *N. meningitidis* P_{II} T-loop tracing also indicates a similar conformation to that observed for *E. coli* P_{II} and the T-loop uridylation site (Tyr51) is also conserved.

As discussed by Xu *et al.* (1998), analysis of the total population of available P_{II} sequences shows that the most highly conserved residues map to the P_{II} ATP-binding site, which is formed by the B-loop of one subunit together with the C-loop and sequences at either end of the T-loop from the adjacent subunit (Xu *et al.*, 1998; Schwarzenbacher *et al.*, 2004; the T-loop, B-loop and C-loop clusters are shown in Fig. 1*a*). As expected, the key contact residues identified by this analysis (Gly27, Thr29, Gly35, Lys58, Gly87, Gly89, Lys90, Arg101 and Arg103) are conserved in the *N. meningitidis* P_{II} sequence and the crystal structure shows they form a pocket equivalent to that seen in *E. coli* (Fig. 1*c*), indicating that the *Neisseria* P_{II} protein is likely to bind to ATP. Analysis of mutants (Jiang, Zucker, Atkinson *et al.*, 1997) and the mode of binding of the inhibitor 2-oxo-3-pentynoate to 4-oxalocrotonate tautomerase (Taylor *et al.*, 1998) have also previously been combined to suggest that Gly37, Arg38, Gln39, Lys40, Thr83, Gly84, Gly89, Lys90 and Arg101 form the 2-oxoglutarate binding site (Machado Benelli *et al.*, 2002). As can be seen in Fig. 1(*a*), all of these residues are conserved in the *N. meningitidis* P_{II} sequence apart from Thr83, which has undergone a neutral mutation to Ser83, thus indicating that the *Neisseria* P_{II} protein is also likely to bind 2-oxoglutarate.

In addition to these features, our analysis of multiple *ClustalW* alignments using sets of sequences from diverse species such as those illustrated in Fig. 1(*a*) has revealed a number of other patterns. Firstly, apart from residues such as Thr29 or Gly35, which are involved in both ATP binding and oligomerization, most residues forming oligomerization contacts are not strictly conserved across the whole population of P_{II} proteins; in part, this reflects the fact that many such contacts are formed between backbone atoms such that the nature of the side chain does not substantially affect the oligomerization. However, for the remaining contacts that do involve side-chain interactions then, as seen by Machado Benelli and coworkers in their comparison of the *H. seropedicae* and *E. coli* GlnK structures, each pair of structures compared does have some contacts in common (Machado Benelli *et al.*, 2002). P_{II} oligomerization-interface contacts therefore tend to show clustering of residue type, with significantly retarded genetic drift relative to the mean difference, *e.g.* the central oligomerization contact between Lys/Arg60 and Asp/Glu62 (Fig. 1*d*). This pattern suggests a strong selective pressure for maintaining the viability of normal trimer formation, which is in line with expectation as such an assembly is believed to be important for the function of P_{II} proteins (Zhang *et al.*, 2004). Secondly, when the residues not involved in ATP or 2-oxyglutarate binding but showing >80% identity are mapped onto our crystal structure, they outline a hydrophobic pocket on the other side of the β-sheet to the ATP-binding site,

together with Ile7 on the same face as the ATP site (Fig. 1*d*). This pattern is strongly conserved, implying that there is a functional significance to the arrangement. It is possible that the conserved residues define a binding site for an unknown ligand. Since the potential pocket is on the opposite side of the β-sheet to the ATP site, such a ligand might function as an allosteric effector regulating P_{II} function by modulating access to the ATP-binding site. An alternative and more speculative interpretation is that the conserved residues are important in stabilizing a conformational change in the molecule. Such a change might occur during interaction with partner proteins. In this case, the hydrophobic side chains currently separated from one another and forming an open pocket might be brought into contact, forming an interdentate cross-link and making the P_{II} protein significantly more rigid.

The interacting partners of the P_{II} in *Neisseria* are currently unknown. However, given the structural conservation of the protein, some candidates can be proposed based on *E. coli* GlnB/GlnK. The genomes of *Neisseriae* encode putative UTase (*e.g.* NMB1203, 31% sequence identity to *E. coli*) and GS-ATase enzymes (*e.g.* NMB0224, 35% sequence identity to *E. coli*) and we suggest that these interact with *N. meningitidis* P_{II}. The nature of the downstream effectors that functionally correspond to *E. coli* NRI/NRII in *Neisseria* spp. is less clear. The likely candidates are the co-transcribed genes that encode NtrX and NtrY (NMB0114/NMB0115), although NtrY only shows 24% sequence identity to *E. coli* NRII. Interestingly, the *Neisseria* NtrY protein is very similar (45% sequence identity) to another 2-component regulator, the *atoS* gene in the related species *Chromobacterium violaceum*. In *E. coli*, AtoS regulates the expression of AtoC involved in short-chain fatty-acid metabolism. In *C. violaceum*, which has both PII and GlnK homologues, *atoS* is located adjacent to *ntrX* in the genome, reminiscent of *NtrB*/*NtrC* in *E. coli* and *NtrX*/*NtrY* in *Neisseria* species. Since *Neisseria* spp. do not appear to have separate *NtrA*, *NtrB*, *atoS* and *atoC* genes, we speculate that the single *N. meningitidis* P_{II} may be involved in the regulation of more than one sensor system *via* NtrY.

The model for the regulatory role of P_{II} is an example of direct sensing and action in which the mechanism of activation and action is dependent upon the direct modification of the sensing protein rather than upon the transcriptional control of the protein itself. Consistent with this, transcriptional profiling normally does not detect the transcript from this gene unless very high data depths (>80%) are obtained, suggesting that it is a relatively low-abundance transcript. Furthermore, it is seldom shown to alter its expression, with the only observed changes to date being between early-log and late-log and between mid-log and late-log phase cultures, but these changes are between 1.9-fold and 1.4-fold induction and are not highly significant ($p < 0.05$) (unpublished observations). This suggests that this gene is induced in conditions in which protein/amino-acid supply is restricted. A low constitutive expression that does not often change under differing conditions is consistent with its primary regulatory role being controlled by changes in a pre-formed protein.

The Oxford Protein Production Facility is funded by the Medical Research Council UK and is part of the Structural Proteomics in Europe (SPINE) consortium (European Commission Grant No. QLG2-CT-2002-00988).

References

Arcondeguy, T., Jack, R. & Merrick, M. (2001). *Microbiol. Mol. Biol. Rev.* **65**, 80–105.

Brünger, A. T., Adams, P. D., Clore, G. M., DeLano, W. L., Gros, P., Grosse-Kunstleve, R. W., Jiang, J.-S., Kuszewski, J., Nilges, M., Pannu, N. S., Read, R. J., Rice, L. M., Simonson, T. & Warren, G. L. (1998). *Acta Cryst.* D**54**, 905–921.

Cheah, E., Carr, P. D., Suffolk, P. M., Vasudevan, S. G., Dixon, N. E. & Ollis, D. L. (1994). *Structure*, **2**, 981–990.

Chenna, R., Sugawara, H., Koike, T., Lopez, R., Gibson, T. J., Higgins, D. G. & Thompson, J. D. (2003). *Nucleic Acids Res.* **31**, 3497–3500.

Clamp, M., Cuff, J., Searle, S. M. & Barton, G. J. (2004). *Bioinformatics*, **20**, 426–427.

Collaborative Computational Project, Number 4 (1994). *Acta Cryst.* D**50**, 760–763.

Coutts, G., Thomas, G., Blakey, D. & Merrick, M. (2002). *EMBO J.* **21**, 536–545.

Forchhammer, K. & Tandeau de Marsac, N. (1995). *J. Bacteriol.* **177**, 2033–2040.

Heeswijk, W. C. van, Hoving, S., Molenaar, D., Stegeman, B., Kahn, D. & Westerhoff, H. V. (1996). *Mol. Microbiol.* **21**, 133–146.

Heeswijk, W. C. van, Stegeman, B., Hoving, S., Molenaar, D., Kahn, D. & Westerhoff, H. V. (1995). *FEMS Microbiol. Lett.* **132**, 153–157.

Heeswijk, W. C. van, Wen, D., Clancy, P., Jaggi, R., Ollis, D. L., Westerhoff, H. V. & Vasudevan, S. G. (2000). *Proc. Natl Acad. Sci. USA*, **97**, 3942–3947.

Humphrey, W., Dalke, A. & Schulten, K. (1996). *J. Mol. Graph.* **14**, 33–38.

Jaggi, R., van Heeswijk, W. C., Westerhoff, H. V., Ollis, D. L. & Vasudevan, S. G. (1997). *EMBO J.* **16**, 5562–5571.

Jaggi, R., Ybarlucea, W., Cheah, E., Carr, P. D., Edwards, K. J., Ollis, D. L. & Vasudevan, S. G. (1996). *FEBS Lett.* **391**, 223–228.

Jiang, P., Peliska, J. A. & Ninfa, A. J. (1998*a*). *Biochemistry*, **37**, 12782–12794.

Jiang, P., Peliska, J. A. & Ninfa, A. J. (1998*b*). *Biochemistry*, **37**, 12795–12801.

Jiang, P., Zucker, P., Atkinson, M. R., Kamberov, E. S., Tirasophon, W., Chandran, P., Schefke, B. R. & Ninfa, A. J. (1997). *J. Bacteriol.* **179**, 4342–4353.

Jiang, P., Zucker, P. & Ninfa, A. J. (1997). *J. Bacteriol.* **179**, 4354–4360.

Jones, T. A., Zou, J. Y., Cowan, S. W. & Kjeldgaard, M. (1991). *Acta Cryst.* A**47**, 110–119.

Laskowski, R. A., MacArthur, M. W., Moss, D. S. & Thornton, J. M. (1993). *J. Appl. Cryst.* **26**, 283–291.

Little, R., Reyes-Ramirez, F., Zhang, Y., van Heeswijk, W. C. & Dixon, R. (2000). *EMBO J.* **19**, 6041–6050.

Liu, J. & Magasanik, B. (1995). *J. Bacteriol.* **177**, 926–931.

Machado Benelli, E., Buck, M., Polikarpov, I., Maltempi de Souza, E., Cruz, L. M. & Pedrosa, F. O. (2002). *Eur. J. Biochem.* **269**, 3296–3303.

Mangum, J. H., Magni, G. & Stadtman, E. R. (1973). *Arch. Biochem. Biophys.* **158**, 514–525.

Martinez-Argudo, I. & Contreras, A. (2002). *J. Bacteriol.* **184**, 3746–3748.

Ninfa, A. J. & Atkinson, M. R. (2000). *Trends Microbiol.* **8**, 172–179.

Ninfa, A. J. & Jiang, P. (2005). *Curr. Opin. Microbiol.* **8**, 168–173.

Otwinowski, Z. & Minor, W. (1997). *Methods Enzymol.* **276**, 307–326.

Parkhill, J. *et al.* (2000). *Nature (London)*, **404**, 502–506.

Ren, J., Sainsbury, S., Berrow, N. S., Alderton, D., Nettleship, J. E., Stammers, D. K., Saunders, N. J. & Owens, R. J. (2005). *BMC Struct. Biol.* **5**, 13.

Sakai, H., Wang, H., Takemoto-Hori, C., Kaminishi, T., Yamaguchi, H., Kamewari, Y., Terada, T., Kuramitsu, S., Shirouzu, M. & Yokoyama, S. (2005). *J. Struct. Biol.* **149**, 99–110.

Schwarzenbacher, R. *et al.* (2004). *Proteins*, **54**, 810–813.

Taylor, A. B., Czerwinski, R. M., Johnson, W. H. Jr, Whitman, C. P. & Hackert, M. L. (1998). *Biochemistry*, **37**, 14692–14700.

Tettelin, H. *et al.* (2000). *Science*, **287**, 1809–1815.

Thompson, J. D., Higgins, D. G. & Gibson, T. J. (1994). *Nucleic Acids Res.* **22**, 4673–4680.

Walter, T. S., Diprose, J. D., Brown, J., Pickford, M., Owens, R. J., Stuart, D. I. & Harlos, K. (2003). *J. Appl. Cryst.* **36**, 308–314.

Xu, Y., Carr, P. D., Clancy, P., Garcia-Dominguez, M., Forchhammer, K., Florencio, F., Vasudevan, S. G., Tandeau de Marsac, N. & Ollis, D. L. (2003). *Acta Cryst.* D**59**, 2183–2190.

Xu, Y., Carr, P. D., Huber, T., Vasudevan, S. G. & Ollis, D. L. (2001). *Eur. J. Biochem.* **268**, 2028–2037.

Xu, Y., Cheah, E., Carr, P. D., van Heeswijk, W. C., Westerhoff, H. V., Vasudevan, S. G. & Ollis, D. L. (1998). *J. Mol. Biol.* **282**, 149–165.

Zhang, Y., Pohlmann, E. L. & Roberts, G. P. (2004). *Proc. Natl Acad. Sci. USA*, **101**, 2782–2787.